Strain broadening of the dangling-bond resonance at the (111)Si-SiO_2 interface

K. L. Brower
Sandia National Laboratories, Albuquerque, New Mexico 87185
(Received 16 September 1985)

It is observed that the linewidth and line shape of the Zeeman resonance associated with dangling bonds at the (111)Si-SiO_2 interface (P_b centers) vary with the direction of the applied magnetic field. An analysis of the line shape of this resonance indicates that it can be represented analytically by the Voigt function, which is a convolution of Lorentzian and Gaussian line broadening. To a first approximation the Lorentzian component is attributed to natural line broadening and is angle independent. The Gaussian component arises from strain broadening of only $g_\perp$ and not $g_{||}$ giving an angle-dependent Gaussian linewidth. The strain broadening of the $\overleftrightarrow{g}$ dyadic is understood in terms of the molecular-orbital theory for the $\overleftrightarrow{g}$ anisotropy of paramagnetic dangling bonds in silicon of Watkins and Corbett. The standard deviation in the bond angle between the paramagnetic dangling bond and the adjacent bonds localized on the common silicon atom is 0.5°, as deduced from our previous measurements of the ^{29}Si hyperfine broadening. It is observed at K band that the relative intensity of the P_b resonance, as determined by double numerical integration of the measured derivative spectrum or from integration of the Voigt function, varies from 1 for $\mathbf{B}||[111]$ to approximately 1.7 for $\mathbf{B}||[1\bar{1}0]$ with $\mathbf{B}_{\text{microwave}}||[11\bar{2}]$.

I. INTRODUCTION

Paramagnetic resonance studies have elucidated numerous features in the structure of the paramagnetic dangling bond at the (111)Si-SiO_2 interface. This specific defect, originally called the P_b center by Nishi[1] who first observed the resonance, was later identified by Caplan, Poindexter, Deal, and Razouk[2] in their electron-paramagnetic-resonance (EPR) studies of thermal oxides on silicon. The fact that the charge state of this defect could be made to vary under the influence of an applied or imposed electric field[3,4,5] emphasized its potential impact on electrical properties. Further studies have in fact shown that this specific defect also dominates the effects of charge trapping at the interface.[4,6] This defect is created or altered by ionizing events[7,8,9,10] and passivated by hydrogen.[11] The complexity of physical and chemical conditions that create or involve this defect make it both scientifically interesting and technologically important. One of the greatest impediments to the investigation of this center, not only by EPR but by many other experimental techniques, is imposed by its very low concentration: the surface density of these centers at the (111)Si-SiO_2 interface is only several times 10^{12} cm^{-2}, and even less in the case of the (001)Si-SiO_2 interface.[12]

This paper addresses yet another aspect of the dangling bond: the effect of strain broadening of the dangling-bond resonance at the (111)Si-SiO_2 interface. The effects of strain are manifested by a variation in the linewidth and line shape of the P_b Zeeman resonance as a function of the direction of the applied magnetic field and excess broadening of the ^{29}Si hyperfine lines. The results of a detailed computer analysis of the line shape of the P_b Zeeman resonance in terms of the Voigt function, which is a convolution of Lorentzian and Gaussian broadening, are presented in Sec. III A. The unusually large angular variation in the linewidth is shown to be due to strain broadening of only $g_\perp$ and not $g_{||}$. The strain broadening of the $\overleftrightarrow{g}$ dyadic is understood in terms of molecular-orbital theory for the $\overleftrightarrow{g}$ anisotropy of dangling bonds in silicon developed by Watkins and Corbett (Sec. III B). We then proceed to deconvolute the Zeeman resonance in terms of its natural and strain-broadened components (Sec. III C). The strain-broadened portion of the Zeeman resonance is, in turn, represented by a distribution in $g_\perp$ (Sec. III D). Finally, a description of the variation in the atomic structure of the P_b center is deduced from the various effects of strain broadening (Sec. III E).

The overall objective of this work is to determine various features in the atomic structure of this interface defect from an analysis of its EPR spectrum. We begin by presenting our experimental approach to this study (Sec. II). A summary of our conclusions is presented in Sec. IV.

II. EXPERIMENTAL

A. Sample preparation

Thin silicon samples measuring 60 μm thick and having a (0.226×2.32) cm^2 (111) face were fabricated from intrinsic vacuum-float-zone silicon (p type, 2000 Ω cm). Each silicon substrate was oriented such that the 2.32-cm edge was a $[11\bar{2}]$ direction and the 0.226-cm edge was a $[1\bar{1}0]$ direction. The (111) faces on both sides of each sample had been cupric-ion electrochemically polished. No near-surface impurities could be detected with Rutherford-backscattering (RBS) measurements; however, a weak resonance near $g=2.0$ was detected with EPR and eliminated by a 4000-Å Sirtl etch.[13,14]

After etching, these silicon samples were oxidized at

900 °C for 1000 min in dry O_2 at a pressure of 1.2×10^5 Pa. During oven warm-up and cool-down, the oxidation tube was back-filled with Ar gas at a pressure of 1.2×10^5 Pa. The thickness of the SiO_2 was 2300 Å as measured by ellipsometry and RBS.

In order to enhance the signal-to-noise ratio in our EPR measurements, 35 of these samples were stacked together, making a bar measuring $0.21\times0.23\times2.32$ cm^3 that was mounted on the axis of a copper TE_{011} cylindrical microwave cavity (cavity diameter equals cavity height equals 1.93 cm). Although the crystalline structure of the silicon substrate is slightly different depending upon whether the sample is mounted with the $[11\bar{2}]$ direction "up" or "down" in the bundle, the EPR spectra of defects associated with the silicon substrate and having symmetry C_s or higher are invariant with respect to this distinction. The symmetry of the P_b center is C_{3v}. This sample bundle was held together by epoxy glue spread over the extreme ends of the sample; these ends were not contained within the microwave cavity. The Si-SiO_2 interface area within the microwave cavity was 30.5 cm^2. This particular sample bundle is, in fact, the same one that was used in our ^{29}Si hyperfine studies of the P_b center.[15]

B. EPR measurements

The EPR measurements of the P_b resonance were made with a K-band (20 GHz) superheterodyne spectrometer[16] in the absorption mode under conditions of adiabatic slow passage. Phase-sensitive detection was used to detect the magnetic-field-modulated resonance so that the recorded spectrum corresponded to the derivative of the absorption resonance. The amplitude of the magnetic field modulation was constrained to levels for which the signal response was proportional to the amplitude of the magnetic field modulation. To enhance our signal-to-noise ratio for the line-shape analyses, the EPR signal was also signal-averaged. To avoid introducing erroneous spectral traces to the accumulated average, the deviation between the new trace and the previously averaged signal was calculated; any deviations outside of what was expected statistically resulted in the new trace being omitted from the accumulated average. A typical signal-averaged spectrum consisted of an average of 25 to 50 traces.

EPR measurements were made at 35, 100, and 250 K. The relative intensity of the P_b resonance is plotted in Fig. 1 as a function of microwave power, temperature, and direction of the applied magnetic field **B**. The data in Fig. 1 show that at 100 K saturation of the P_b resonance appears to begin at about -33 dBm (0.5 μW) for a cavity Q of about 13 000; this is evidenced in Fig. 1 by the decrease in the intensity for microwave powers in excess of -36 dBm (0.25 μW) at 100 K. Another significant effect is that the intensity depends on the direction of the applied magnetic field; in Fig. 1 the solid data points correspond to the intensity $I_{||}$ taken with the magnetic field parallel to the [111] direction ($\theta=0°$), and the open data points correspond to the intensity $I_\perp$ taken with **B** perpendicular to the [111] direction ($\theta=90°$). At 100 K the average ratio in $I_\perp/I_{||}$, which is referred to in this paper as the intensity anisotropy factor, was 1.75 at 19.747 GHz. To assure ourselves that this was not due to the effects of saturation arising from an angular anisotropy in the spin-lattice relaxation times, intensity measurements were also made at 250 K (Fig. 1). Measurements at 250 K indicated that the intensity anisotropy factor was 1.69, and at 35 K it was approximately 2.0. (At 35 K, interference with weak background resonances is believed to have caused the intensity anisotropy factor to be enhanced.) These results were independent of the rotational orientation of the sample bundle about the cylindrical axis of the microwave cavity. The intensity of the P_b resonance was normalized with respect to the signal intensity from a powdered, isotropic spin standard at each magnet angle. For a simple spin-$\frac{1}{2}$ system, the intensity anisotropy factor calculated from the transition probabilities is 1 for our configuration of magnetic fields. The physical basis for this larger-than-expected anisotropy in intensity remains unknown at this time; however, similar effects of this nature have been observed previously. Watkins and Corbett[17] called attention to this effect in their EPR studies of the divacancy in silicon; we also noticed this effect on our studies of the Si-$B3$ center (see Fig. 3 of Ref. 18). Until this effect is better understood, measurements of the spin density should be qualified with respect to the direction of **B** and the measured intensity anisotropy factor, which might be microwave-frequency dependent.

Since this particular study dealt extensively with the line shape of the P_b resonance as a function of the direction of the applied magnetic field, we were concerned about the sensitivity of the line shape to variations in microwave power, temperature, and the effects of partial saturation. For purposes of comparison a line-shape factor was arbitrarily defined as the peak amplitude of the ab-

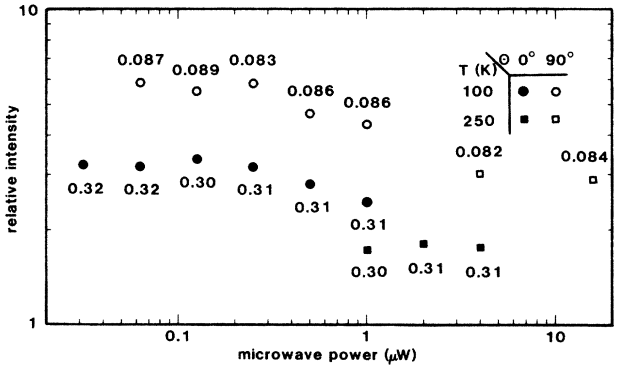

FIG. 1. Plot of the relative intensity of the P_b Zeeman resonance versus microwave power as a function of magnet angle [which is defined in Fig. 2(a)] and temperature. The numbers associated with the data points are a measure of the line shape, which is defined as the peak amplitude of the absorption resonance divided by the area under the absorption resonance. The area was determined by double numerical integration of the derivative of the absorption. The relative intensity is equal to the (numerical area)$\times$[temperature (K)] $\times(10^{-\text{microwave power (dBm)}/20})$/[(cavity Q)$\times$(B modulation)]. If the spin density were constant with no saturation and if the intensity anisotropy factor were 1, the data points would lie on a single horizontal line.

sorption resonance, corresponding to the integrated derivative spectrum, divided by the area of the absorption resonance. This line-shape factor, which has the units of G^{-1}, is quoted by the data points in Fig. 1 and indicates that the line shape for each direction of **B** was insensitive to variations in temperature, microwave power, and the effects of partial saturation.

III. ANALYSIS AND INTERPRETATION

A. Deconvolution of the P_b resonance in terms of Lorentzian and Gaussian components

Inspection of the spectra in Fig. 2(b) due to P_b centers at the (111)Si-SiO_2 interface indicates that the peak-to-peak derivative linewidth of this resonance varies with the direction of the applied magnetic field. Computer analyses of these resonances indicate that their line shape varies from nearly Lorentzian for **B** perpendicular to the interface to an admixture of Gaussian and Lorentzian for **B** in the plane of the interface.[19] For **B** perpendicular to the interface, one notices satellite structure which is believed to be due to partially resolved ^{29}Si superhyperfine spectra; therefore, this resonance line is not believed to derive its general Lorentzian-like character from lifetime-broadening effects, but is an inhomogeneously broadened resonance.

The Gaussian and Lorentzian admixture in the line shape of the P_b resonance suggested to us that its line shape might be well represented by the Voigt function[20]

$$Y(v,b)=\frac{Ab}{\pi}\int_{-\infty}^{+\infty}\frac{e^{-x^2}dx}{b^2+(v-x)^2}\ , \tag{1a}$$

where

$$v=\sqrt{2}\frac{B-B_0}{\Delta B_{pp}^G} \tag{1b}$$

and

$$b=\left[\frac{3}{2}\right]^{1/2}\frac{\Delta B_{pp}^L}{\Delta B_{pp}^G}\ . \tag{1c}$$

The Voigt function represents the convolution of Lorentzian and Gaussian broadening. In Eq. (1a), B_0 is the center of the resonance, ΔB_{pp}^L is the Lorentzian peak-to-peak derivative linewidth, ΔB_{pp}^G is the Gaussian peak-to-peak derivative linewidth, and A is the relative intensity of the resonance.

The derivative of the Voigt function with respect to the magnetic field, dY/dB, plus a baseline function, which was simply a second-order polynomial in $B-B_0$, was least-squares-fitted to between 200 and 300 data points evenly selected from the observed, signal-averaged P_b resonance. All seven parameters were allowed to vary in the least-squares fit. The peak-to-peak Gaussian and and Lorentzian linewidths resulting from the least-squares-fit analysis are shown in Fig. 3.

The results of least-squares fitting the derivative with respect to B of the Voigt, Gaussian, and Lorentzian functions to the P_b resonance for several directions of **B** are summarized in Table I. Also included is the relative intensity obtained from double integration of the derivative spectra in Fig. 2(b). There is reasonably close agreement between the relative intensities determined from the Voigt function and double numerical integration of the observed resonance which indicates that the Voigt function is a reasonable approximation to the absorption resonance. By comparison, the disparity in the relative intensities of the Lorentzian and Gaussian functions illustrates their inadequacy. The significantly larger standard deviations in the least-squares fit of the analytical functions to the observed spectra for $\theta=0°$ is due to the effects of partially resolved satellite structure, which smears out as the direction of **B** is tilted from this high-symmetry direction. Calculated spectra corresponding to the derivative of the Voigt function with respect to B as deduced from this least-squares-fitting procedure are represented in Fig. 2(b) by the dots.

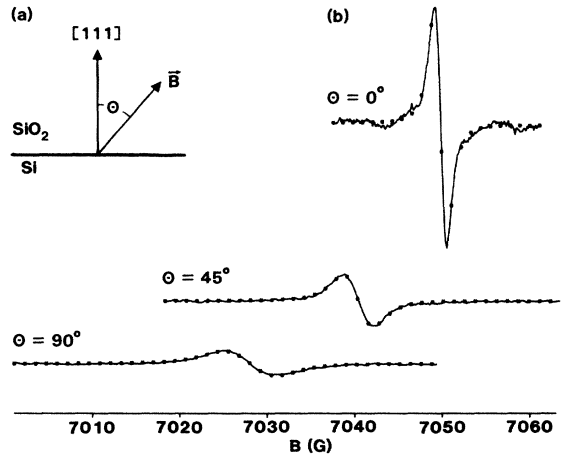

FIG. 2. (a) Definition of the magnet angle θ. (b) EPR spectra of the P_b resonance observed at K-band frequency (19.752 GHz) at 100 K with a microwave power of -33 dBm. The sensitivity of the vertical scale is the same for these three resonances. The dots correspond to the calculated Voigt line shape resulting from a least-squares-fit analysis (see Table I).

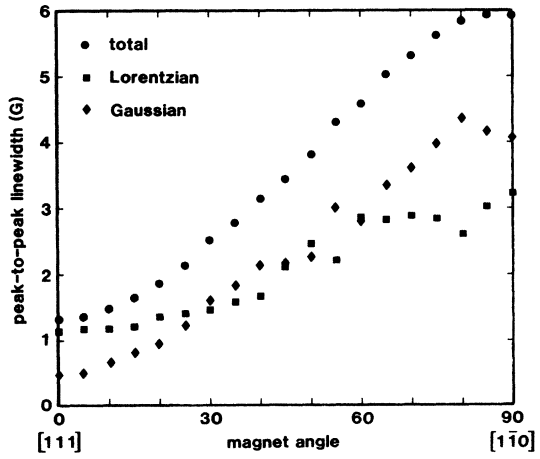

FIG. 3. Plot of the Gaussian and Lorentzian peak-to-peak linewidths deduced from a least-squares fit of the Voigt function to the experimentally observed spectra at 100 K as a function of the magnetic field direction. The total peak-to-peak linewidth was determined from Eq. (4).

TABLE I. Tabulation of the linewidths, relative intensities, and relative standard deviation as a function of the method of analysis and the magnet angle. The experimental spectra used in this analysis are shown in Fig. 2(b). Relative intensities and relative standard deviations are directly comparable in this table.

Analysis	θ (deg)	ΔB_{pp}^{T} (G)	ΔB_{pp}^{L} (G)	ΔB_{pp}^{G} (G)	Relative intensity	Relative standard deviation
Least-squares fit	0	1.33	1.14	0.49	3.25	4.8
of Voigt function	45	3.44	2.11	2.14	3.45	1.2
	90	5.94	3.20	4.03	4.49	0.8
Least-squares fit	0		1.27		3.51	5.0
of Lorentzian function	45		3.10		4.44	1.6
	90		5.30		6.23	1.0
Least-squares fit	0			1.58	1.58	10.7
of Gaussian function	45			3.83	1.98	2.0
	90			6.54	2.73	1.0
Numerical	0				3.19	
integration	45				3.75	
	90				4.85	

B. Atomic origin of the $\vec{\vec{g}}$ anisotropy for dangling bonds

Previous analyses of the P_b Zeeman spectrum[2] and the ^{29}Si hyperfine (hf) spectrum[15] indicate the P_b center observed from the (111)Si-SiO_2 interface is due to an unpaired electron mostly localized within a [111] dangling bond on a threefold-coordinated substitutional Si atom on the silicon side of the Si-SiO_2 interface. The hyperfine interaction indicates that 80% of the spin density is localized on this interfacial Si atom and that this hybrid orbital is 12% s-like and 88% $p_{[111]}$-like. Prior to our ^{29}Si hyperfine measurements, Redondo, Goddard III, McGill, and Surratt[21] predicted from self-consistent Hartree-Fock and generalized valence-bond calculations of the Si_4H_9 cluster model of the (111)Si surface that 93.1% of the paramagnetic dangling bond was localized in the region of the defect surface atoms with 92.9% $p_{[111]}$-like character. The P_b center has C_{3v} symmetry within the accuracy of the EPR measurements, as evidenced by the sharpness and lack of any apparent splitting in the resonance line for $\theta=0°$. This means that in the case of the (111)Si-SiO_2 interface the dangling bond is essentially perpendicular to the interface and does not reflect any other surface irregularities such as adjacent ledges or atomic steps[22] as part of the immediate structure of the P_b center. The C_{3v} symmetry of this defect also probably rules out the existence of an oxygen atom in any one or two of the three covalent bonds common with the Si atom on which the dangling bond is highly localized, since this could perturb the C_{3v} symmetry of the defect to a measurable and discrete degree.

Several well-known defects observed in bulk silicon similarly have dangling bonds localized on a single substitutional Si atom adjacent to a vacancy, namely the phosphorous vacancy (Si-$G8$) (Ref. 23) and the negative 5-vacancy complex (Si-$P1$) (Ref. 24) centers. Watkins and Corbett[23] have shown, using simple molecular-orbital theory, that the anisotropy in the $\vec{\vec{g}}$ dyadic for such a dangling bond is axial about the direction of the dangling bond with

$$g_{||}=g_{\text{free}} \tag{2}$$

and

$$g_{\perp}=g_{\text{free}}+\Delta g_{\perp} , \tag{3a}$$

where

$$\Delta g_{\perp}\cong\lambda_{3p}\left[\frac{1+\gamma}{E_b}-\frac{1-\gamma}{E_a}\right]\beta^2 \tag{3b}$$

and

$$\gamma=-\frac{\lambda_{2p,3p}\epsilon_{2p}}{\lambda_{3p}\beta} . \tag{3c}$$

Here ϵ_{2p} is an overlap integral, and the λ_i correspond to spin-orbit constants; γ has a value of approximately 0.17.[23] Measurements of the $\vec{\vec{g}}$ dyadic for the P_b center indicate that $g_{||}=2.0016$ and $g_{\perp}=2.0090$ (Refs. 2, 12, and 15), with axial symmetry about the [111] direction perpendicular to the (111)Si-SiO_2 interface. The important point here is that $g_{||}$ is—to a first approximation—unperturbed by lattice interaction ($g_{\text{free}}=2.0023$), whereas $g_{\perp}$ depends on β^2, the amount of $p_{[111]}$-like character in the dangling bond, and E_a and E_b, the defect antibonding and bonding energy levels, respectively. The direct consequence of this interaction with the surrounding lattice is that slight variations in bond length and angles in the neighborhood of this defect produce a distribution in $g_{\perp}$ which is manifested by increased Zeeman broadening of the resonance line as the direction of **B** approaches the plane of the interface [see Fig. 2(b)].

C. Deconvolution of the P_b resonance in terms of natural and strain-broadened components

In attempting to deconvolute the observed resonance into its natural and strain-broadened components, several approximations are made. The first approximation is that the natural line shape corresponds to the observed P_b resonance observed at $\theta=0°$ since $\Delta g_\perp=0$ (no strain broadening possible). The results of our analysis in Table I indicate that the natural line shape is mostly Lorentzian with a linewidth of 1.3 G. The presence of partially resolved ^{29}Si superhyperfine interactions suggests that the natural broadening is dominated by ^{29}Si hyperfine interactions. Although the partially resolved ^{29}Si superhyperfine structure associated with the EPR spectra of deep-level defects typically sharpens and blends as the magnetic field direction changes from high to low symmetry, the natural linewidth of the main resonance remains essentially independent of the magnetic field direction. With regard to the line shape, Feher[25] found that for shallow donors in silicon the line shape of the donor resonance is Gaussian. He also observed that if the number of ^{29}Si nuclei with which the electron overlaps is greatly reduced by isotopic ^{28}Si doping, the linewidth is significantly reduced and the line shape is observed to tend toward being Lorentzian. For deep-level defects the paramagnetic wave function is much more localized than it is for shallow donors, so that, in effect, the linewidth is reduced and might deviate from Gaussian. In the case of the P_b resonance, the existence of partially resolved ^{29}Si superhyperfine spectra is evidence against the P_b resonance being exchange-narrowed; however, it is conceivable that the Lorentzian component might, in part, be due to the additional effects of exchange interactions between P_b centers whose paramagnetic wave functions overlap. Preliminary calculations indicate that the natural line shape may also be affected by dipolar interactions between the unpaired electrons at the interface. In view of these considerations, we have allowed the natural component of the total line shape to be Lorentzian with constant linewidth equal to that of the observed resonance at $\theta=0°$.

The second approximation is that the strain component of the linewidth is purely Gaussian. The effects of strain broadening have been observed previously from defects in glasses.[26] The physically most meaningful approach is to allow for a Gaussian distribution in some atomic structure parameters, e.g., energy-level splittings, which then convolute into some distribution in the elements of the $\overleftrightarrow{g}$ dyadic. However, the electronic structure of the P_b center is not sufficiently well defined within this sort of theoretical context to arrive at an unambiguous distribution in $g_\perp$. If the natural resonance has a 1.33-G Lorentzian component, then the remaining 1.87 G of the total Lorentzian linewidth for $\theta=90°$ (3.20 G in Table I) contributes to the distribution in strain broadening. Thus in reality, the strain component of the linewidth, which if represented analytically, is dominated by Gaussian with a small admixture of Lorentzian.[27] In our approximation the strain component of the linewidth is purely Gaussian.

Implicit in the analysis which follows is the idea that the line shape is still reasonably well approximated by the Voigt function in which the Lorentzian broadening corresponds to the natural linewidth and the Gaussian broadening represents broadening due to strain.

Stoneham[28] has established a simple empirical relationship between the total, Lorentzian, and Gaussian linewidths of the Voigt function, which is

$$\Delta B_{pp}^{T}=\frac{(\Delta B_{pp}^{G})^2+0.9085(\Delta B_{pp}^{G})(\Delta B_{pp}^{L})+0.4621(\Delta B_{pp}^{L})^2}{\Delta B_{pp}^{G}+0.4621(\Delta B_{pp}^{L})}\ , \tag{4}$$

and accurate to better than $0.01\Delta B_{pp}^{T}$ for all ΔB_{pp}^{G} and ΔB_{pp}^{L}.

The total linewidth observed from data taken at 100 and 35 K, respectively, was deconvoluted using Eq. (4), in which the natural linewidth was totally ascribed to a constant Lorentzian component and a Gaussian component attributed to Zeeman broadening due to strain. The results of this deconvolution are shown in Figs. 4 and 5.

D. Characterization of strain in terms of $\delta g_\perp$

The analyzed data points in Figs. 4 and 5 show that ΔB_{pp}^{G} due to strain has a distinct angular variation. We will now show that this experimentally observed angular variation in ΔB_{pp}^{G} can be related to the Gaussian distribution in $g_\perp$ according to the following. The position of the Zeeman resonance is given by

$$B=h\nu/\mu_B g\ , \tag{5a}$$

where

$$g=[(g_{||}\cos\theta)^2+(g_\perp\sin\theta)^2]^{1/2}\ . \tag{5b}$$

In Eq. (5a), μ_B is the Bohr magneton and ν is the microwave frequency; in Eq. (5b), θ is the angle between **B** and the [111] direction perpendicular to the interface [see Fig. 2(a)]. Since the derivative of B in Eq. (5a) with respect to $g_\perp$ is

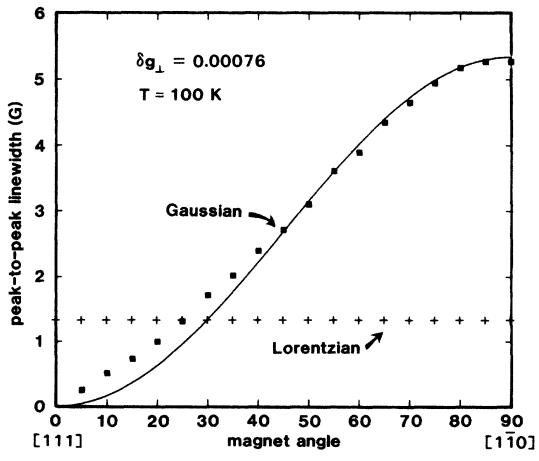

FIG. 4. Plot of the peak-to-peak Gaussian linewidth as function of the direction of the applied magnetic field assuming a fixed peak-to-peak Lorentzian linewidth of 1.33 G as deduced from the total linewidth of spectra taken at 100 K using Eq. (4).

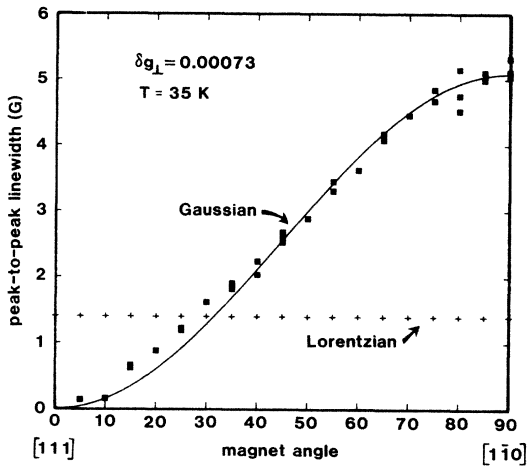

FIG. 5. Plot of the peak-to-peak Gaussian linewidth as function of the direction of the applied magnetic field assuming a fixed peak-to-peak Lorentzian linewidth of 1.4 G as deduced from the total linewidth of spectra taken at 35 K using Eq. (4).

$$\frac{dB}{dg_\perp} = -\frac{h\nu g_\perp \sin^2\theta}{\mu_B g^3} , \tag{6a}$$

it is our contention that the peak-to-peak linewidth of the Gaussian component representing strain broadening of the resonance line and $\delta g_\perp$, the standard deviation in $g_\perp$, are—to a first approximation—related by the expression

$$\Delta B_{pp}^G = \frac{2h\nu g_\perp \sin^2\theta}{\mu_B g^3}\delta g_\perp . \tag{6b}$$

The standard deviation in $g_\perp$ for a Gaussian distribution is defined within the context of the function

$$\frac{1}{\sqrt{2\pi}\delta g_\perp}\exp\{-\tfrac{1}{2}[(g_\perp - \langle g_\perp\rangle)/\delta g_\perp]^2\} .$$

The value for $\delta g_\perp$ was found by least-squares-fitting the analyzed data points in Figs. 4 and 5 to Eq. (6b); the results of this least-squares-fit analysis are well represented by the solid line in Figs. 4 and 5, which was calculated according to Eq. (6b). The average value for the standard deviation in $g_\perp$ is given by[29]

$$\delta g_\perp = 0.00075 \pm 0.0001 . \tag{7}$$

The extent to which this value for $\delta g_\perp$ in Eq. (7) characterizes all (111)Si-SiO_2 oxides has not yet been established, but it has appeared to be essentially constant for a variety of dry oxides that we have grown on (111)Si.

Equation (6b) also indicates that the Zeeman broadening arising from a Gaussian distribution in $g_\perp$ is linearly dependent on the microwave frequency, whereas the Lorentzian component due to hyperfine broadening is frequency independent (to a first approximation). At 9 GHz (X-band frequency) the total peak-to-peak linewidth is predicted by our analysis [Eqs. (4), (6b), and (7)] to vary from 1.3 G for **B** perpendicular to the interface to 3.07 G for **B** parallel to the interface. This is, in fact, consistent with the earlier observation of Poindexter, Ahlstrom, and Caplan,[30] who noted that at X band frequency ($\approx$9 GHz) the peak-to-peak linewidth varied from 1 G for **B** perpendicular to the (111)Si-SiO_2 to 3 G for **B** in the plane of the (111)Si-SiO_2 interface.

Although the density of unpaired spins on the (111)Si-SiO_2 interface is approximately 0.5% of the [111] Si—O bonding sites, we have as yet not been able to identify a contribution to the angular variation in the linewidth due to magnetic-dipole—dipole interactions between the spins.[31]

E. Variations in bond angles

According to simple molecular-orbital theory[32] the angle ξ between the dangling bond $\alpha|s\rangle+\beta|p\rangle$ and the adjacent sp^3 hybrid bonding orbitals localized on the same silicon atom, illustrated in Fig. 6, is

$$\cos\xi = -\left[\frac{\alpha^2}{3\beta^2}\right]^{1/2} . \tag{8}$$

If the strain distribution in $g_\perp$ were totally attributed to the variation in β^2 in Eq. (3b), then the standard deviation in the bonding angle ξ among different P_b centers would be approximately 5°. This is equivalent to a rms variation in the vertical position of the defect Si atom of 0.2 Å. This is regarded as an *extreme upper limit* in the distortion since the total variation in $g_\perp$ should also depend on variations in the bonding and antibonding energies in Eq. (3b). Evidence for variation in the energy level structure of the P_b center can be seen from Fig. 7 of Ref. 6. Due to the limitations in the theory which relates the $\vec{g}$ to the atomic structure of the defect, our numerical estimates of the strain as deduced here should be regarded as approximate.

The existence of strain at the interface is also corroborated by excess line broadening of the P_b ^{29}Si hyperfine resonances.[15] Each distinct ^{29}Si hyperfine interaction which can be measured yields values for α^2 and β^2 as well as $\delta(\alpha^2)$ and $\delta(\beta^2)$ for that specific site;[33] therefore the excess hyperfine broadening provides a more direct and specific indication of the variation in the bonding angle ξ in Fig. 6 than that deduced from the distribution in $g_\perp$. We have not performed a detailed line-shape analysis of the ^{29}Si hyperfine lines, as we have done in this paper for the Zeeman resonance, since the ^{29}Si hyperfine spectrum is very much weaker. However, our previous estimates of $\delta(\alpha^2)$ and $\delta(\beta^2)$ determined from the excess broadening of the ^{29}Si hyperfine lines due to strain[15] indicate that the

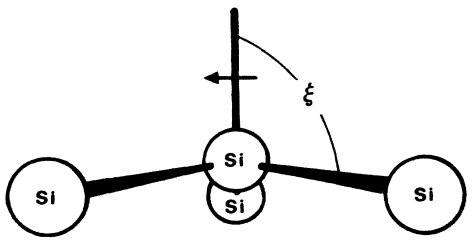

FIG. 6. Basic structure of the P_b center and the definition of the bonding angle ξ.

standard deviation in ξ is approximately 0.5°, which corresponds to an rms variation in the vertical position of the defect Si atom of 0.02 Å. The nature of the strain is such as to preserve the C_{3v} symmetry of the individual P_b centers within the limits of our resolution.

The magnitude of the atomic displacements around the P_b center at the (111)Si-SiO_2 interface as inferred from EPR are somewhat less than the magnitude of the distortions determined from channeling studies of the (111)Si-SiO_2 interface which indicate that the first two silicon monolayers next to the interface are displaced laterally ≈ 0.1 Å and vertically ≈ 0.2 Å.[34] In making comparisons between the EPR and channeling results, it should be remembered that the channeling measurements can sample all of the crystalline Si atoms at the interface, whereas the EPR measurements sample only a subset of Si atoms in an environment described above (Sec. III B). Also, these defect Si atoms are trivalently bonded, which might also account for some difference in the degree of local distortion.

Finally, Redondo, Goddard III, McGill, and Surratt[21] have shown from self-consistent Hartree-Fock and generalized valence-bond calculations of the Si_4H_9 cluster model that the angle ξ in Fig. 6 depends on the charge state of the surface defect. For the neutral paramagnetic charge state the defect Si atom relaxes inward -0.08 Å from its tetrahedral position toward the bulk. In the positive diamagnetic charge state the defect Si atom relaxes inward -0.38 Å from the tetrahedral position, and in the negative diamagnetic charge state the defect Si atom relaxes outward $+0.17$ Å from the tetrahedral position. Recently, Edwards also arrived at similar conclusions from linear combination of atomic orbitals—molecular-orbital calculations.[35] The variation in ξ due to strain as deduced from our EPR studies is smaller than the deviations in ξ corresponding to changes in charge state.

IV. SUMMARY AND CONCLUSIONS

This work presents the results of our study of the paramagnetic dangling Si bond at the (111)Si-SiO_2 interface (P_b center) using electron paramagnetic resonance. We find that the excess broadening of the P_b spectrum is dominated by the effects of strain in the neighborhood of the dangling-bond defect. The magnitude of the distortion as deduced from the excess broadening of the ^{29}Si hyperfine spectra which we have studied previously[15] indicates that the rms variation in the bonding angle ξ shown in Fig. 6 is 0.5°. This corresponds to a rms variation in the vertical position of the defect Si atoms on the silicon "surface" at the interface of approximately 0.02 Å. The effects of strain in the immediate neighborhood of the P_b center are also responsible for broadening of the Zeeman resonance, which is dependent on the direction of the applied magnetic field. The Zeeman broadening due to strain is characterized by a Gaussian distribution in $g_\perp$ having a rms variation of $0.000\,75 \pm 0.0001$;[29] $g_{||}$ is insensitive to the effects of strain and remains constant. The difference in sensitivity of the various elements in the $\overleftrightarrow{g}$ dyadic to strain are understood in terms of molecular-orbital theory (Sec. III B). The magnitude of the distortion as deduced from strain broadening of the Zeeman resonance indicates that the rms variation in the vertical position of the defect Si atom is <0.2 Å.

In our analysis the Zeeman line was least-squares-fitted to the Voigt function, which is a convolution of Lorentzian and Gaussian broadening. To a first approximation the natural linewidth, which is dominated by ^{29}Si superhyperfine broadening and is approximately independent of the direction of the applied magnetic field, is represented by the Lorentzian portion of the Voigt function, with a Lorentzian peak-to-peak derivative linewidth of between 1.3 and 1.4 G. The broadening due to strain, which is dependent on the direction of the applied magnetic field, is approximately represented by the Gaussian portion of the Voigt function, whose linewidth is given by Eqs. (6b) and (7). Although the density of spins on the (111)Si-SiO_2 interface is approximately 0.5% of the [111] Si—O bonding sites, no contribution to the angular variation in the linewidth due to magnetic-dipole—dipole interactions between the spins has yet been detected.

The intensity of the P_b resonance for this spin-$\frac{1}{2}$ system is expected to be invariant with respect to the direction of the applied magnetic field for the case in which the applied magnetic field is perpendicular to the microwave magnetic field. However, our measurements at ≈ 20 GHz indicate that the relative intensity of the P_b resonance as determined by double numerical integration of the observed derivative spectrum or from integration of the Voigt function varies from 1 for $\mathbf{B}||[111]$ to approximately 1.7 for $\mathbf{B}||[1\bar{1}0]$ with $\mathbf{B}_{\text{microwave}}||[11\bar{2}]$. This effect is not understood at this time.

ACKNOWLEDGMENTS

The expert assistance of Roger Shrouf with the EPR measurements and sample preparation is gratefully acknowledged. The Rutherford-backscattering measurements referred to in Sec. II were made by Dr. S. T. Picraux. Several software programs were provided by Dr. J. A. Knapp and discussions with him have been very helpful. Discussions with Dr. E. L. Venturini and Dr. S. M. Myers, who reviewed this paper, are greatly appreciated. This work was performed at Sandia National Laboratories and was supported by the U. S. Department of Energy under Contract No. DE-AC04-76DP00789.

[1] Y. Nishi, Jpn. J. Appl. Phys. **10**, 52 (1971).

[2] P. J. Caplan, E. H. Poindexter, B. E. Deal, and R. R. Razouk, J. Appl. Phys. **50**, 5847 (1979).

[3] C. Brunström and C. Svensson, Solid State Commun. **37**, 399 (1981).

[4] P. M. Lenahan and P. V. Dressendorfer, Appl. Phys. Lett. **41**, 542 (1982).

[5] N. M. Johnson, D. K. Biegelsen, M. D. Moyer, and S. T. Chang, Appl. Phys. Lett. **43**, 563 (1983).

[6] E. H. Poindexter, G. J. Gerardi, M.-E. Rueckel, P. J. Caplan, N. M. Johnson, and D. K. Biegelsen, J. Appl. Phys. **56**, 2844 (1984).

[7]P. M. Lenahan, K. L. Brower, and P. V. Dressendorfer, IEEE Trans. Nucl. Sci. **NS-28**, 4105 (1981).
[8]K. L. Brower, P. M. Lenahan, and P. V. Dressendorfer, Appl. Phys. Lett. **41**, 251 (1982).
[9]R. E. Mikawa and P. M. Lenahan, Appl. Phys. Lett. **46**, 550 (1985).
[10]P. M. Lenahan and P. V. Dressendorfer, Appl. Phys. Lett. **44**, 96 (1984).
[11]N. M. Johnson, D. K. Biegelsen, and M. D. Moyer, in *The Physics of MOS Insulators,* edited by G. Lucovsky, S. T. Pantelides, and F. L. Galeener (Pergamon, New York, 1980), p. 311; J. Vac. Sci. Technol. **19**, 390 (1981).
[12]E. H. Poindexter, P. J. Caplan, B. E. Deal, and R. R. Razouk, J. Appl. Phys. **52**, 879 (1981).
[13]E. Sirtl and A. Adler, Z. Metallk. **52**, 529 (1961).
[14]R. B. Heiman, J. Mater. Sci. **19**, 1314 (1984).
[15]K. L. Brower, Appl. Phys. Lett. **43**, 1111 (1983).
[16]K. L. Brower, Rev. Sci. Instrum. **48**, 135 (1977).
[17]G. D. Watkins and J. W. Corbett, Phys. Rev. **138**, A543 (1965).
[18]K. L. Brower, Phys. Rev. B **14**, 872 (1976).
[19]In this paper we refer to the "Lorentzian" or "Gaussian" character of the resonance irrespective of whether the resonance corresponds to an absorption resonance or the first derivative of the absorption resonance with respect to magnetic field. Also, all linewidths discussed in this paper and in the formulas are peak-to-peak derivative linewidths.
[20]D. W. Posener, Aust. J. Phys. **12**, 184 (1959).
[21]A. Redondo, W. A. Goddard III, T. C. McGill, and G. T. Surratt, Solid State Commun. **20**, 733 (1976).
[22]J. H. Mazur and J. Washburn, in *Physics of VLSI,* edited by J. C. Knights (AIP, New York, 1984).
[23]G. D. Watkins and J. W. Corbett, Phys. Rev. **134**, A1359 (1964).
[24]Y.-H. Lee and J. W. Corbett, Phys. Rev. B **8**, 2810 (1973).
[25]G. Feher, Phys. Rev. **114**, 1219 (1959).
[26]D. L. Griscom, J. Non-Cryst. Solids **31**, 241 (1978).
[27]We have also carried out an analysis in which the natural linewidth is Lorentzian and constant and the strain component is a composite of Lorentzian and Gaussian. Although this is a more precise representation, it is algebraically more complex and gives in the final analysis nearly the same result, namely $\delta g_{\perp}=0.000\,81$.
[28]A. M. Stoneham, J. Phys. D **5**, 670 (1972).
[29]In Refs. 15 and 31, a value for $\delta g_{\perp}$ of about twice this value is quoted and corresponds to approximately the peak-to-peak Gaussian width in the variation of $g_{\perp}$. The rms variation quoted in this paper is one-half of the peak-to-peak Gaussian width.
[30]E. H. Poindexter, E. R. Ahlstrom, and P. J. Caplan, in *The Physics of* SiO_2 *and its Interfaces,* edited by S. T. Pantelides (Pergamon, New York, 1978), p. 227.
[31]K. L. Brower, in *13th International Conference on Defects in Semiconductors,* edited by L. C. Kimerling and J. M. Parsey, Jr. (The Metallurgical Society of AIME, Warrendale, PA, 1985), p. 485.
[32]C. A. Coulson, *Valence* (Oxford University Press, London, 1961), p. 203.
[33]K. L. Brower, Phys. Rev. B **20**, 1799 (1979).
[34]R. Haight and L. C. Feldman, J. Appl. Phys. **53**, 4884 (1982).
[35]A. H. Edwards, in *13th International Conference on Defects in Semiconductors,* Ref. 31, p. 491.